Analytical computation of free vibration modes : application to non rigid motion analysis and animation in 3D images

Chahab Nastar

350 ex

INRIA

INSTITUT NATIONAL DE RECHERCHE EN INFORMATIQUE ET EN AUTOMATIQUE

Analytical Computation of the Free Vibration Modes : Application to Non Rigid Motion Analysis and Animation in 3D Images

Chahab NASTAR

N° 1935
Juin 1993

PROGRAMME 4

Robotique, image
et
vision

Rapport de recherche

1993

Analytical Computation of the Free Vibration Modes : Application to Non Rigid Motion Analysis and Animation in 3D Images

Chahab NASTAR

INRIA – Rocquencourt

B.P. 105

78153 Le Chesnay Cédex, France

e-mail: Chahab.Nastar@inria.fr

Programme 4

Robotique, Image et Vision

Abstract

In this paper, we concentrate on non rigid motion analysis and synthesis in $3D$ images using modal dynamics.

Using the solid state physics formulation, we develop the analytic expression of eigenmodes of the multidimensional elastically-deformable model exposed in our previous publications. These analytic expressions are calculated for various topologies (plane, cylinder, torus).

Thanks to these expressions, non rigid motion of a $3D$ deformable object can be approximated in modal space in *real time*, by superimposing a few number of low-frequency modes that can be computed in a straightforward manner, *whatever the size of the structure.*

The power of the approach for analyzing $3D$ non rigid motion is demonstrated by a set of experimental results on a $3D$ time sequence of the human heart. Then the heart is animated between the diastole and the systole.

Real-time animation capturing a high level of details is shown on a $3D$ magnetic resonance head data.

Finally, the contribution of this paper is making modal analysis an efficient and easy-to-use tool for non rigid motion analysis and animation.

Calcul analytique des modes propres de vibration : application à l'analyse de mouvement et à l'animation dans les images tridimensionnelles

Résumé :

Nous présentons la dynamique modale pour l'analyse de mouvement ou l'animation d'objets d'objets déformables dans les images $3D$. En utilisant le formalisme de la physique du solide, nous développons l'expression analytique des modes propres de vibration du modèle élastique exposé dans nos publications antérieures. Ces expressions sont calculées pour différentes topologies (plane, cylindrique, torique). Grâce à ces expressions, le mouvement non rigide d'un objet déformable tridimensionnel peut être approximé en temps réel *dans l'espace modale, en superposant quelques modes de basse fréquence qui sont calculés directement,* indépendammant de la taille de la structure. *La puissance de notre approche pour analyser le mouvement non rigide $3D$ est démontré par des résultats expérimentaux sur une séquence d'images $3D$ du coeur humain. Ce coeur est ensuite animé entre la diastole et la systole. Nous présentons également un exemple temps réel d'animation sur un bloc de données $3D$ de tête. Enfin, la contribution de cet article est de faire de l'analyse modale un outil puissant et efficace pour l'analyse du mouvement non rigide et pour l'animation.*

1 Modal Analysis : a summary

In the deformable model described in our previous publications [5, 6, 7, 8], we have exposed the modal analysis of a macroscopic elastic model, governed by a second-order ordinary differential matrix equation of order N [1] :

$$M\ddot{U} + C\dot{U} + KU = F_t \tag{1}$$

We have shown that if we solve the generalized eigenproblem :

$$K\phi = \omega^2 M\phi \tag{2}$$

then we can choose a transformation matrix Φ whose entries are the eigenvectors, and perform a change of basis $U = \Phi\tilde{U}$. The new modal basis simultaneously diagonalizes M and K, and, provided that C is also diagonal in this basis, the problem is simplified, and we solve the decoupled equations :

$$\ddot{\tilde{u}}_i(t) + \tilde{c}_i\dot{\tilde{u}}_i(t) + \omega_i^2\tilde{u}_i(t) = \tilde{F}_i(t) \qquad i = 1, \ldots, N. \tag{3}$$

The decomposition of nodal displacements U in the modal space is then :

$$U(t) = \Phi\tilde{U} = \sum_{i=1}^{N} \tilde{u}_i(t)\phi_i \tag{4}$$

But most of the time only a small number p of low-frequency modes are superimposed, as they can quite accurately recover the motion :

$$U(t) \approx \sum_{i=1}^{p} \tilde{u}_i(t)\phi_i \qquad p \ll N \tag{5}$$

[1] in this paper K and M refer to stiffness and mass constants (scalars) or matrices, k being the wave vector

2 Motivations for deriving the analytic expression of eigenmodes

Even as a precalculation, solving the generalized eigenproblem is costly as soon as we consider surfaces. For instance, if we consider a 100 × 100 patch, the value of N is 10000, that is to say, *a generalized eigenproblem, where the size of the matrices is 10000 × 10000, has to be solved.* It is then clear that the analytic expression of the modes would noticeably reduce the precalculations. Moreover, we want a better physical understanding of the modes. Are they related to Fourier analysis and wave propagation? This leads us to consider the solid states physics theory, where similar type of problems are encountered at a microscopic level (ionic vibrations of a crystal lattice [1, 3, 4]). This is the reason why in the next sections we will often refer to the nodes as ions or atoms.

3 The harmonic approximation

The classical theory of vibration of a crystal lattice is based on two assumptions :

1. The mean equilibrium position of each ion is a "Bravais" lattice. This allows the definition of R as the mean position of the ion about which the ion oscillates.

2. The typical excursion of each ion from its equilibrium position are small compared with the interionic spacing. This leads to the *harmonic approximation*, from which precise quantitative results can be extracted.

More precisely, let $r(R)$ the present position of the ion whose mean position is R :

$$r(R) = R + u(R)$$

The total potential energy of the crystal is the sum of the contributions of all distinct pairs :

$$V = \frac{1}{2}\sum_{R,R'} v(r(R) - r(R')) = \frac{1}{2}\sum_{R,R'} v(R - R' + u(R) - u(R')) \tag{6}$$

If all the $u(R) - u(R')$ are small, we expand the potential energy V about its equilibrium value, using the three dimensional form of Taylor theorem :

$$V = \frac{N}{2}\sum_{R} v(R) + \frac{1}{2}\sum_{R,R'} (u(R) - u(R'))\nabla v(R - R') + \frac{1}{4}\sum_{R,R'} ((u(R) - u(R')).\nabla)^2 v(R - R') + O(u^3) \tag{7}$$

The coefficient of $u(R)$ in the linear term is $\sum_{R'} \nabla v(R - R')$. This is minus the force exerted on the atom R by all other atoms, when each is placed at its equilibrium position. It must therefore vanish, since there is no net force on any atom in equilibrium.

Thus, the first nonvanishing correction to the equilibrium potential energy is given by the quadratic term :

$$V = V^{eq} + V^{harm}$$

where :

$$V^{harm} = \frac{1}{4}\sum_{\substack{R,R' \\ \mu,\nu}} (u_\mu(R) - u_\mu(R'))v_{\mu\nu}(R - R')(u_\nu(R) - u_\nu(R'))$$

$$v_{\mu\nu}(r) = \frac{\partial^2 v(r)}{\partial r_\mu \partial r_\nu}$$

$$\mu, \nu = x, y, z$$

The harmonic potential energy is usually written in the more general form :

$$V^{harm} = \frac{1}{2}\sum_{\substack{R,R' \\ \mu,\nu}} u_\mu(R) D_{\mu\nu}(R - R') u_\nu(R') \tag{8}$$

4 Energy based formulation of the motion

In this section we derive the motion of a three dimensional lattice under external load F by an energy-based approach. This formulation is an alternative to the force-based formulation as described in [6].

4.1 Governing equations

In the case of free vibrations, the motion of the point defined by R lattice in the μ direction ($\mu = x, y$ or z) is defined by :

$$M\ddot{u}_\mu(R) + \frac{\partial V^{harm}}{\partial u_\mu(R)} = 0$$

Considering external load F and damping force, this expression is modified to :

$$M\ddot{u}_\mu(R) + C\dot{u}_\mu(R) + \frac{\partial V^{harm}}{\partial u_\mu(R)} = F_\mu(R)$$

where V^{harm} has the general expression defined by equation (8). This equation yields :

$$M\ddot{u}_\mu(R) + C\dot{u}_\mu(R) + \sum_{R',\nu} D_{\mu\nu}(R - R')u_\nu(R') = F_\mu(R)$$

In a three-order matrix form :

$$M\ddot{u}(R) + C\dot{u}(R) + \sum_{R'} D(R - R')u(R') = F(R) \tag{9}$$

Note that, for the whole lattice, N matrix equations of the above type are to be solved. Each one of these differential equations is *linear*, but nodal displacements are *coupled* in space positions (the nodes) and directions (the axes).

4.2 Properties

The D matrices have the following properties :

- Symmetry 1 : $D_{\mu\nu}(R-R') = D_{\nu\mu}(R'-R)$. This follows from the general definition of $D_{\mu\nu}(R-R')$ as a second derivative of the interaction potential, because of the independence of order of differentiation.

- Symmetry 2 : $D_{\mu\nu}(R-R') = D_{\mu\nu}(R'-R)$, since the harmonic potential is unchanged by replacement $u(R) \rightarrow -u(-R)$.

- Symmetry 3 : $\forall \mu, \nu \sum_R D_{\mu\nu}(R) = 0$. If every ion is given the same displacement, then the entire crystal will simply be translated without internal distortion ($V^{harm} = 0$).

4.3 Unification

Let us concentrate now on the connection between the above formulation and the force-based formulation described in our previous publications. We can rewrite the N equations (9) as one $3N$ order matrix equation :

$$M\ddot{U} + C\dot{U} + \mathcal{D}U = F \tag{10}$$

where matrice $\mathcal{D}$ is constituted by submatrices whose properties are described in section 4.2.

A stiffness matrice K as defined in [6] is a particular matrix $\mathcal{D}$, where the submatrices $D(R-R')$ are all 3×3 diagonal matrices. These submatrices obey the properties listed in the last section. This is why the equations of motion that we have used in [6] can be seen in the harmonic approximation framework, with the further assumption : *a nodal motion in the μ direction exerts a force on the node's neighbors in the same μ direction.*

One of the other advantages of the energy-based formulation with the harmonic approximation is that it avoids the introduction of equilibrium forces in the force-based formulation of [6]. Note that no "springs" are introduced in the modelling. Of course the forces can

sometimes be seen as spring-like forces, but it is more desirable to see the elasticity of the model in an energetic point of view.

5 Free vibrations of a one-dimensional lattice

Consider a set of ions distributed along a line at points seperated by a distance a, so that the lattice vectors are $R = na$ for $n \in \{1, \ldots, N\}$. If only neighboring ions interact, so we may take the harmonic potential energy to have the form :

$$V^{harm} = \frac{1}{2} K \sum_{n=1}^{N} [u(na) - u((n+1)a)]^2$$

where K = v"(a), v(x) being the interaction energy of two ions a distance x along the line. The free vibrations of the lattice are governed by :

$$M\ddot{u}(na) = -\frac{\partial V^{harm}}{\partial u(na)} = K(u((n+1)a) + u((n-1)a) - 2u(na)) \tag{11}$$

These are precisely the equations that would be obeyed if each ion were connected to its neighbors by perfect massless springs of stiffness K (and equilibrium length a, although the equations are in fact independent of the equilibrium length of the spring). The lattice can be either a closed or an open chain.

5.1 Closed chain

In this section we concentrate on a closed chain of N elements. The periodicity of the chain is expressed by the Born-von Karman condition :

$$u[(n+N)a] = u(na) \tag{12}$$

We seek solutions to equation (11) of the form :

$$u(na, t) = Ae^{i(kna - \omega t)} \tag{13}$$

The Born-von Karman condition requires that :

$$e^{ikNa} = 1$$

that is :

$$k_p a = \frac{2p\pi}{N} \qquad p \in \mathcal{Z}$$

Note that if k is changed by $2\pi/a$, the displacement $u(na)$ defined by (13) is unaffected, Consequently, there are just N values of k that yield distinct solutions. We take them to be values between $-\pi/a$ and π/a, thus defining the first Brillouin Zone.

$$\begin{cases} p \in \mathcal{FBZ} = \{-\frac{N}{2}+1, \ldots, \frac{N}{2}\} & N \text{ even} \\ p \in \mathcal{FBZ} = \{-\frac{N-1}{2}, \ldots, \frac{N-1}{2}\} & N \text{ odd} \end{cases} \tag{14}$$

Substituting (13) into (11) leads to the *dispersion equation* :

$$\omega^2 = \frac{4K}{M}\sin^2(\frac{ka}{2}) \tag{15}$$

$$\omega = 2\sqrt{\frac{K}{M}}|\sin(\frac{ka}{2})| \tag{16}$$

As the values of k are discrete, the vibration states of the crystal are discretized. This is the concept of *phonons* in solid state physics. The representation of ω as a function of k is known as the dispersion curve (see figure 1).

An arbitrary motion of the chain can be expressed by the linear combination of the former solutions :

$$u(na,t) = \sum_{p\in\mathcal{FBZ}} A_p e^{i(k_p na - \omega_p t)} \tag{17}$$

The motion is fully determined by specifying N initial positions and N initial velocities of the ions.

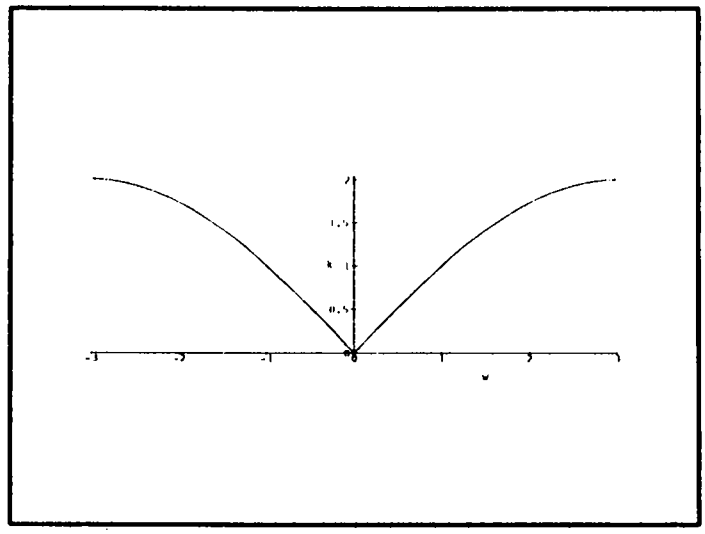

Figure 1: Dispersion curve of a closed chain (N=6)

In mathematical terms, this equation can be seen as the Fourier expansion of the displacement in the basis of the complex exponential functions of period N. In a physics point of view, the solutions describes waves propagating along the chain with phase velocity ω/k and group velocity $\partial\omega/\partial k$.

5.2 Open chain

In the case of an open chain the calculations are slightly different because of the boundary conditions :

$$M\ddot{u}(na) = K(u((n+1)a) + u((n-1)a) - 2u(na)) \quad (18)$$

$$M\ddot{u}(a) = K(u(2a) - u(a)) \quad (19)$$

$$M\ddot{u}(Na) = K(u((N-1)a) - u(Na)) \quad (20)$$

We search for time dependencies of the form $e^{-i\omega t}$, which yields the same dispersion equation than in the case of a closed chain :

$$\omega^2 = \frac{4K}{M} \sin^2(\frac{ka}{2}) \tag{21}$$

For these more complex equations, we seek specific solutions of a more general form :

$$u(na,t) = e^{-i\omega t}(Ae^{ikna} + Be^{-ikna}) \tag{22}$$

Substituting this equation into boundary equations, and remembering the dispersion equation, we obtain :

$$k_p a = \frac{p\pi}{N} \tag{23}$$

$$B = Ae^{ika} \tag{24}$$

For the exponentials to take all possible independent values, we must ensure $0 \leq kNa \leq \pi$, i.e. :

$$p \in \{0, \ldots, N-1\}$$

The specific solutions are now modified to :

$$u(na,t) = Ae^{-i\omega t}e^{i\frac{ka}{2}} cos(kna - \frac{ka}{2}) \tag{25}$$

An arbitrary motion of the chain can be expressed by the linear combination of the former solutions :

$$u(na,t) = \sum_{p=0}^{N-1} A_p e^{-i\omega_p t}e^{i\frac{k_p a}{2}} cos(k_p na - \frac{k_p a}{2}) \tag{26}$$

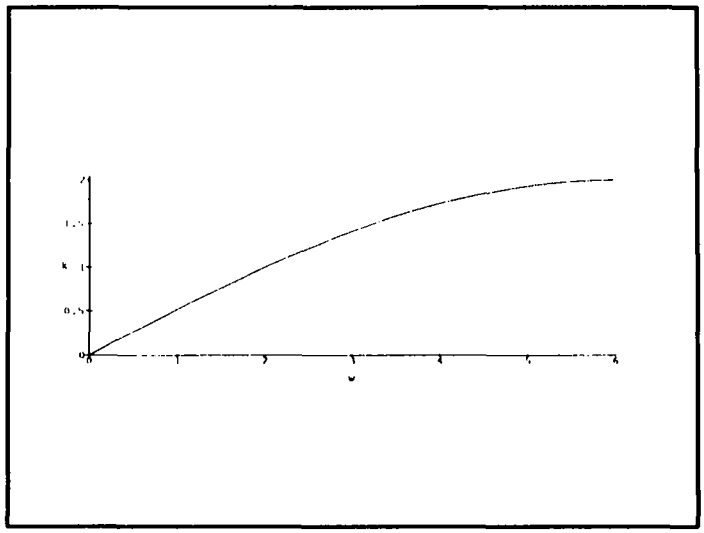

Figure 2: Dispersion curve of an open chain (N=6)

6 Nonlinear waves in discrete media

When k is small compared with π/a (i.e., when the wavelength is large compared with the interparticle spacing), ω is linear in k :

$$\omega = a\sqrt{\frac{K}{M}}|k| \tag{27}$$

This is the type of behavior we are accustomed to in the case of light waves and ordinary sound waves. If ω is linear in k, then the group velocity is the same as the phase velocity (equal to $c = a\sqrt{\frac{K}{M}}$), and both are independent of frequency. Note that if we approximate finite differences by derivatives :

$$u((n+1)a) - u(na) \simeq a\frac{\partial u}{\partial x}(na)$$

$$u((n-1)a) - u(na) \simeq a\frac{\partial u}{\partial x}((n-1)a)$$

$$u((n+1)a) - u(na) + u((n-1)a) - u(na) \simeq a^2\frac{\partial^2 u}{\partial x^2}$$

in equation (11), we end up with a wave equation of velocity c :

$$\frac{\partial^2 u}{\partial x^2} = \frac{1}{c^2}\frac{\partial^2 u}{\partial t^2} \qquad \text{with} \quad c = a\sqrt{\frac{K}{M}}$$

One of the characteristic features of waves in discrete media, however, is that the nonlinearity ceases to hold at wavelengths short enough to be comparable with the interparticle spacing. In the present case ω falls below ck as k increases, and the group velocity drops to zero when $|k|$ reaches π/a.

7 Connection with the theory of modal analysis

We shall remember that equation (17) holds for the free vibrations of the chain. For a governing equation of type (1), the time dependency of the solution is generally not harmonic, and the solution must be modified into :

$$u(na,t) = \sum_{p \in \mathcal{FBZ}} \tilde{u}_p(t) e^{ik_p na} \tag{28}$$

for a closed chain and :

$$u(na,t) = \sum_{p=0}^{N-1} \tilde{u}_p(t) \cos(k_p na - \frac{k_p a}{2}) \tag{29}$$

for an open chain (we have dropped the term $e^{i\frac{k_p a}{2}}$ which is constant for a given mode p).

The analogy between equation (28) and the modal superposition equation (4) is straightforward provided that we make the modes and the modal amplitudes real numbers.

7.1 Eigenvalues and eigenvectors of a closed chain

The eigenvalues ω_p^2 are defined by the dispersion equation :

$$\omega_p^2 = \frac{4K}{M} \sin^2(\frac{p\pi}{N}) \tag{30}$$

Note that if N is odd, $\omega_0^2 = 0$ is the only simple eigenvalue, all others are double. If N is even, $\omega_0^2 = 0$ and $\omega_{N/2}^2 = 4K/M$ are simple eigenvalues, all others being double.

For simple eigenvalues, the associated eigenvector is the real part of the complex mode in equation (28) :

$$\phi_p = [\cos \frac{2p\pi}{N}, \ldots, \cos \frac{2p\pi n}{N}, \ldots, \cos \frac{2p\pi N}{N}]^T$$

For double eigenvalues, a set of two orthogonal eigenvectors (that we will call cosine and sine modes) can be chosen as :

$$\phi_p = [\cos \frac{2p\pi}{N}, \ldots, \cos \frac{2p\pi n}{N}, \ldots, \cos \frac{2p\pi N}{N}]^T$$

$$\phi_p = [\sin \frac{2p\pi}{N}, \ldots, \sin \frac{2p\pi n}{N}, \ldots, \sin \frac{2p\pi N}{N}]^T$$

7.2 Eigenvalues and eigenvectors of an open chain

The eigenvalues ω_p^2 are defined by the dispersion equation :

$$\omega_p^2 = \frac{4K}{M} \sin^2(\frac{p\pi}{2N}) \tag{31}$$

Note that all eigenvalues are simple. The eigenvectors have the following expression :

$$\phi_p = [\cos(\frac{p\pi}{2N}), \ldots, \cos(\frac{p\pi(2n-1)}{2N}), \ldots, \cos(\frac{p\pi(2N-1)}{2N})]^T$$

7.3 Stationary waves

Consider equation (28). The total displacement appears to be the superposition of terms

$$\tilde{u}_p(t)e^{ik_p na}$$

In this expression, the time dependency and the space dependency are independent (this is also the case for equation (29)). This characterizes a *stationary wave*. There is no propaga-

tion (see figure 3). *Modal analysis corresponds to the decomposition of the displacement in a basis of stationary waves.*

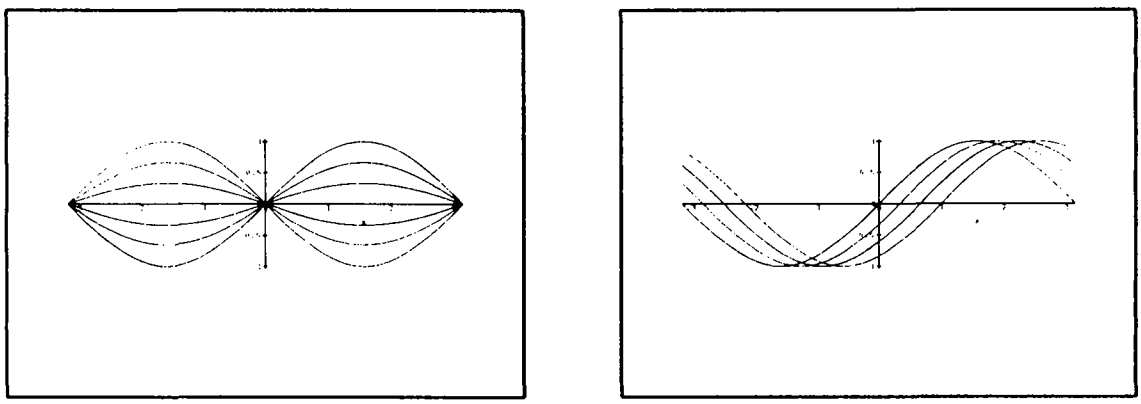

Figure 3: A stationary and a progressive sine wave

8 Dynamical matrix

In this section we expose another method for mode computation. This method has the advantage of solving N eigenproblems of 3×3 matrices instead of one eigenproblem of $3N \times 3N$ matrix. Consider the N matrix equations of free vibration of the $3D$ lattice :

$$M\ddot{u}(R) + \sum_{R'} D(R - R')u(R') = 0 \tag{32}$$

As in the one-dimensional cases we seek solutions to the equations of motion in the form of simple plane waves :

$$u(R, t) = \epsilon \, e^{i(k.R - \omega t)} \tag{33}$$

Here ϵ is a vector, to be determined, that describes the direction in which the ions move. It is known as the polarization vector of the normal mode.

We need a boundary condition, and we simply use the Born-von Karman condition, requiring that $u(R + N_i a_i) = u(R)$ for each of the three primitive vectors a_i, where the N_i

are integers satisfying $N = N_1 N_2 N_3$. This restricts the allowed wave vectors k to those of the form :

$$k = \frac{n_1}{N_1} b_1 + \frac{n_2}{N_2} b_2 + \frac{n_3}{N_3} b_3$$

where the b_i are reciprocal lattice vectors satisfying $b_i a_j = 2\pi\delta_{ij}$. Again, there are only N values of k that yield nonequivalent modes. If we substitute equation (33) into (32), we get the 3 order eigenproblem :

$$D(k)\epsilon = M\omega^2\epsilon \tag{34}$$

Here $D(k)$, known as the dynamical matrix, is given by :

$$D(k) = \sum_R D(R) e^{-ik.R}$$

Using the properties described in section 4.2 :

$$D(k) = \frac{1}{2}\sum_R D(R)[e^{-ik.R} + e^{ik.R} - 2] = \sum_R D(R)[\cos(k.R) - 2]$$

In other terms :

$$D(k) = -2\sum_R D(R)\sin^2(\frac{k.R}{2}) \tag{35}$$

$D(k)$ is an even function of k, and a real symmetric matrix. Its eigenvectors can be normalized to :

$$\epsilon_s \epsilon_{s'} = \delta_{ss'} \qquad s, s' = 1, 2, 3. \tag{36}$$

Evidently the three normal modes eith wave vector k will have polarization vectors $\epsilon_s(k)$ and frequencies $\omega_s(k)$ given by :

$$\omega_s(k) = \sqrt{\frac{\lambda_s(k)}{M}}$$

where $\lambda_s(k), s = 1,2,3$ are the eigenvalues of $D(k)$. There are three dispersion curves, and $\omega_s(k)$ vanish linearly in k for small k, i.e. low-frequency waves are elastic, as in the one-dimensional case.

Let us consider the particular case of stiffness matrices defined in [7]. As outlined before, submatrices $D(R)$ are disgonal in this model. In a $2D$ case, we have :

$$D(R) = \begin{bmatrix} -K & 0 \\ 0 & -K \end{bmatrix} \tag{37}$$

for a closed structure. Substituting $D(R)$ in equation (35) yields :

$$D(k) = \begin{bmatrix} 4K\sin^2(\frac{k.R}{2}) & 0 \\ 0 & 4K\sin^2(\frac{k.R}{2}) \end{bmatrix} \tag{38}$$

In other terms, in the model described in our previous publications, *D(k) is already a diagonal matrix.* Its eigenvalues are its diagonal terms, and the basis vectors are its eigenvectors. The modes are axis-dependent, and described by equation (33).

9 $3D$ Analysis

In this section we consider surface meshes as described in our previous publications (an "inside" node of these meshes has exactly four neighboring nodes).

The $3D$ generalization of the analytic expressions of the modes is straightforward, provided that some topological properties are outlined. In the following subsections, we denote $\vec{k}_{p,p'} = (k_p, k_{p'})$ the wave vector and $\vec{R} = (na, n'a')$ the position vector. The patch of nodes has a size $N \times N'$.

9.1 Torus topology

The torus has the simplest topological properties. There is no boundary, and all the points are topologically equivalent. The Fourier expansion of the displacement is :

$$u(\vec{R},t) = \sum_{p,p' \in \mathcal{FBZ}} A_{p,p'} e^{i(\vec{k}_{p,p'}.\vec{R} - \omega_{p,p'}t)} \tag{39}$$

with :

$$k_p a = \frac{2p\pi}{N} \qquad k_{p'} a' = \frac{2p'\pi}{N'}$$

and :

$$\omega_{p,p'} = \frac{4K}{M}(\sin^2\frac{p\pi}{N} + \sin^2\frac{p'\pi}{N'})$$

This last equation expresses the eigenvalues. The eigenvectors are :

$$\phi_{p,p'} = [\ldots, \cos(\frac{2p\pi n}{N} + \frac{2p'\pi n'}{N'}), \ldots]^T$$

As shown by the dispersion equation, the dimension of the eigenspaces can be equal to four (changing p to $-p$ and/or p' to $-p'$ leaves the eigenvalue $\omega_{p,p'}$ unchanged). A set of orthogonal eigenvectors can be chosen as :

$$\phi_{p,p'} = [\ldots, \cos(\frac{2p\pi n}{N} + \frac{2p'\pi n'}{N'}), \ldots]^T$$

$$\phi_{p,p'} = [\ldots, \sin(\frac{2p\pi n}{N} + \frac{2p'\pi n'}{N'}), \ldots]^T$$

with p and $p' \in \mathcal{FBZ}$.

9.2 Plane topology

The parameters describing a plane topology are submitted to open boundary conditions. The Fourier expansion of the displacement is therefore :

$$u(\vec{R},t) = \sum_{p,p'=0}^{N-1} A_{p,p'} e^{-i\omega_{p,p'}t} \cos(k_p n a - \frac{k_p a}{2}) \cos(k_{p'} n' a' - \frac{k_{p'} a'}{2}) \tag{40}$$

with :

$$k_p a = \frac{p\pi}{N} \qquad k_{p'} a' = \frac{p'\pi}{N'}$$

and :

$$\omega_{p,p'} = \frac{4K}{M}(\sin^2 \frac{p\pi}{2N} + \sin^2 \frac{p'\pi}{2N'})$$

The eigenvalues are all simple. The eigenvectors have the following expression :

$$\phi_{p,p'} = [\ldots, \cos \frac{p\pi(2n-1)}{2N} \cos \frac{p'\pi(2n'-1)}{2N'}, \ldots]^T$$

9.3 Cylinder topology

The Fourier expansion of the displacement is :

$$u(\vec{R}, t) = \sum_{\substack{p=0 \\ p' \in \mathcal{FBZ}}}^{N-1} A_{p,p'} e^{-i\omega_{p,p'} t} \cos(k_p n a - \frac{k_p a}{2}) e^{ik_{p'} n' a'} \tag{41}$$

with :

$$k_p a = \frac{p\pi}{N} \qquad k_{p'} a' = \frac{2p'\pi}{N'}$$

and :

$$\omega_{p,p'} = \frac{4K}{M}(\sin^2 \frac{p\pi}{2N} + \sin^2 \frac{p'\pi}{N'})$$

For simple eigenvalues :

$$\phi_{p,p'} = [\ldots, \cos \frac{p\pi(2n-1)}{2N} \cos \frac{2p'\pi n'}{N'}, \ldots]^T$$

If the eigenvalue is double, a set of orthogonal eigenvectors is :

$$\phi_{p,p'} = [\ldots, \cos \frac{p\pi(2n-1)}{2N} \cos \frac{2p'\pi n'}{N'}, \ldots]^T$$

$$\phi_{p,p'} = [\ldots, \cos \frac{p\pi(2n-1)}{2N} \sin \frac{2p'\pi n'}{N'}, \ldots]^T$$

10 Motion analysis

10.1 Modal approximation

Applications of modal analysis in computer vision have been described in various papers [11, 6]. Once the mode shapes are computed, the equations of motion can be expressed in modal space where their expression is simple, and the nonrigid motion can be approximated by a reduced number of parameters, the modal amplitudes. The accuracy of the approximation is controlled thanks to the number of modal amplitudes.

Figure 4 demontrates the power of modal approximation. On the left, the left ventricle is tracked from the diastole (shown as a mesh) to the systole, via our method. The number of nodes is $100 \times 40 = 4000$. On the right, we have superimposed 20×3 low frequency modes to recover the systole. The factor of compression is then $(4000 \times 3)/(20 \times 3) = 200$. Globally, once the modes are precomputed using the analytic expressions derived in the previous sections, only $20 \times 3 = 60$ scalars, the modal amplitudes, contain the information of deformation from the diastole to the systole. Note that the result of the superposition has roughly the same shape that the original diastole, illustrating the smoothing of the motion. The superposition can be even closer to the real result if we increase the number of modes.

10.2 A diagnosis tool?

Medical imaging appears to be an important field for the application of modes. For instance, for purposes of heart diseases diagnosis, decomposing the heart's motion in the modal basis can reveal certain anomalies in terms of modes, since, during its motion, an anormal heart is expected to have radically different vibration modes than a normal heart. An animation of the ventricle from diastole to systole is shown in figure 5.

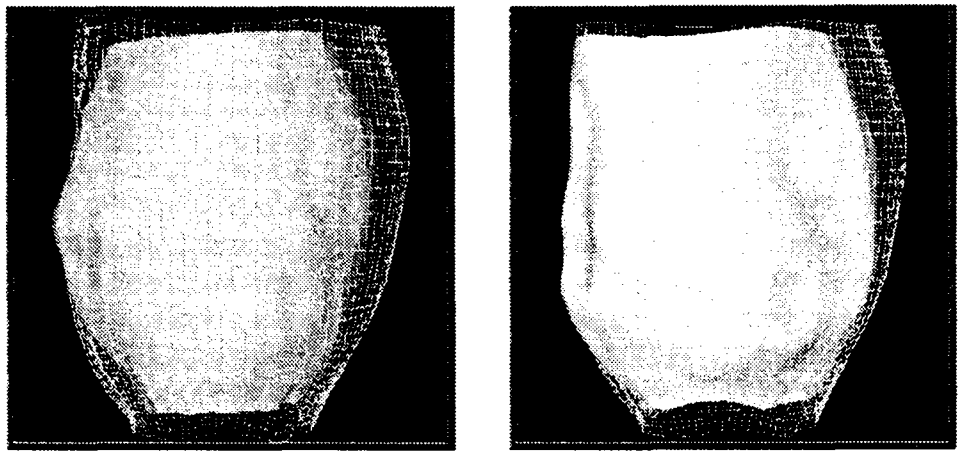

Figure 4: Left : segmented diastole (mesh), tracked to the systole. Right : modal approximation of the motion ; the factor of compression is 200

11 Modes for computer graphics

Mode shapes can be efficiently used in computer graphics as well. Pentland and his colleagues have shown the ability of the modes to synthetize various types of deformations [10, 12].

Using modal dynamics, one can deform a $3D$ object M into M_i' with the i-th mode ϕ_i using the $3N$ order vector equation :

$$M_i' = M + \alpha\phi_i$$

Moreover, if we make the amplitude α time-dependent, we can animate the object through one or several modes. Making the time dependency periodic efficiently simulates the *vibration* of the object around its initial shape.

$$M_i'(t) = M + (\alpha \sin \gamma t)\phi_i$$

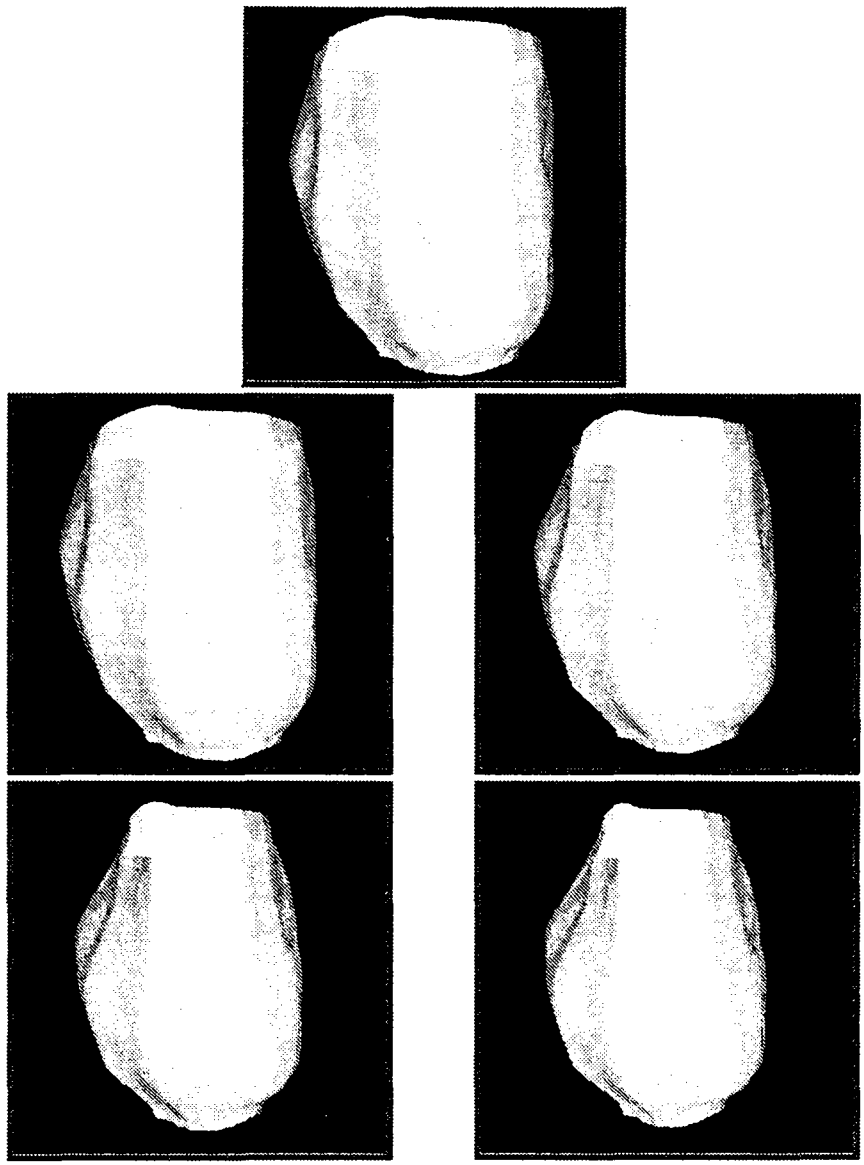

Figure 5: Animating the left ventricle between diastole (top) and systole (bottom, right) by superimposing 60 vibration modes

Such an animation is synthetized in figures 8 and 9. In this figure, a $3D$ magnetic resonance (MR) image of the human head is segmented thanks to our mesh-spring model (see figures 6 and 7). The result is animated thanks to modal dynamics. Note that these

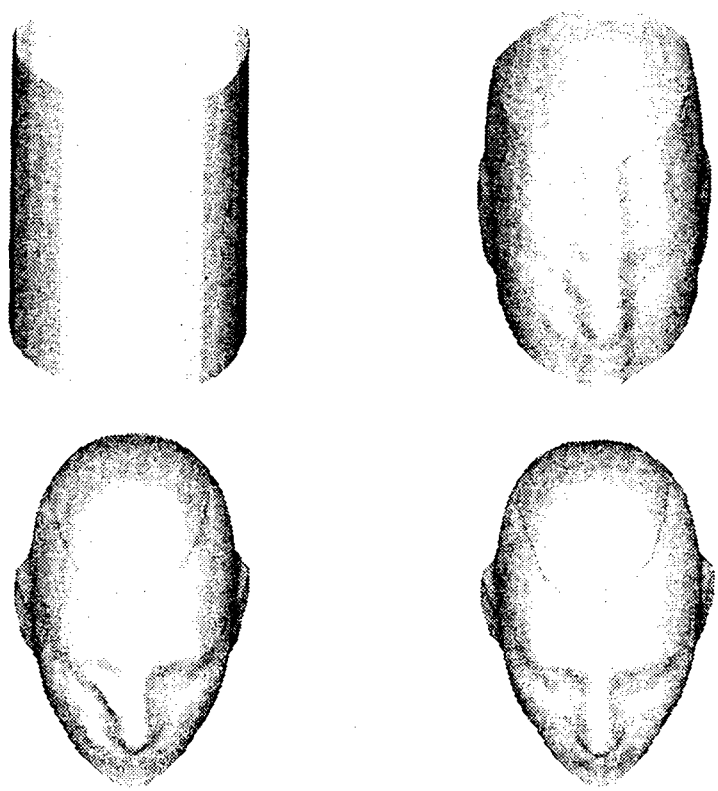

Figure 6: Segmenting the $3D$ MR head by our model

animations are *real time whatever the size of the structure* (here $159 \times 70 = 11130$ nodes) since we make use of an analytic expression of mode shapes. Note that several modes can be superimposed in order to synthetize the desirable shape. For a complex animation, one can choose several suitable modes :

$$M'(t) = M + \sum_i \alpha_i(t)\phi_i$$

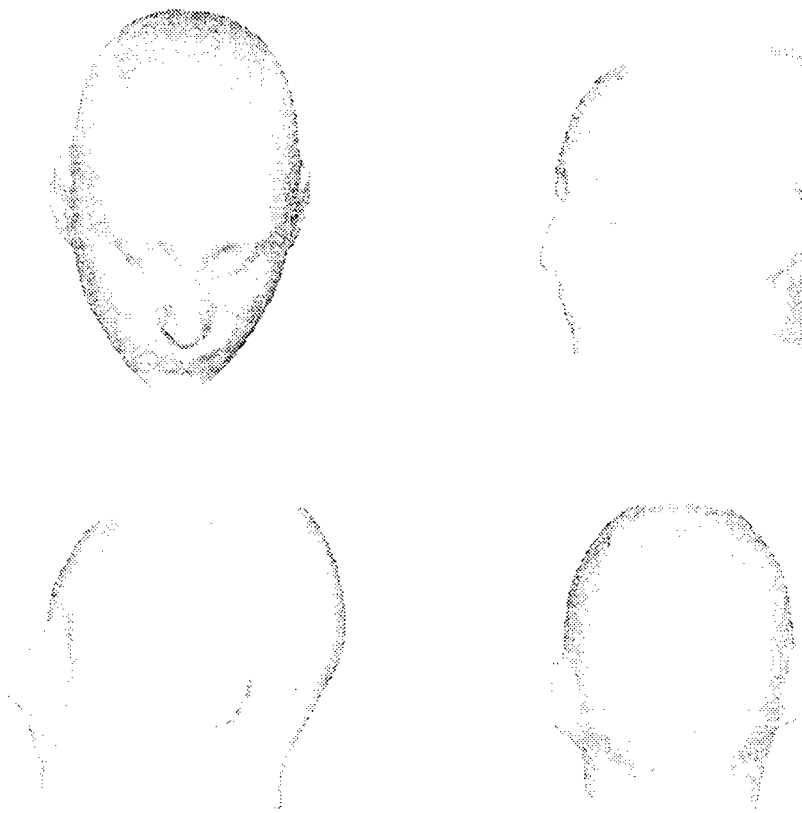

Figure 7: Result of the segmentation

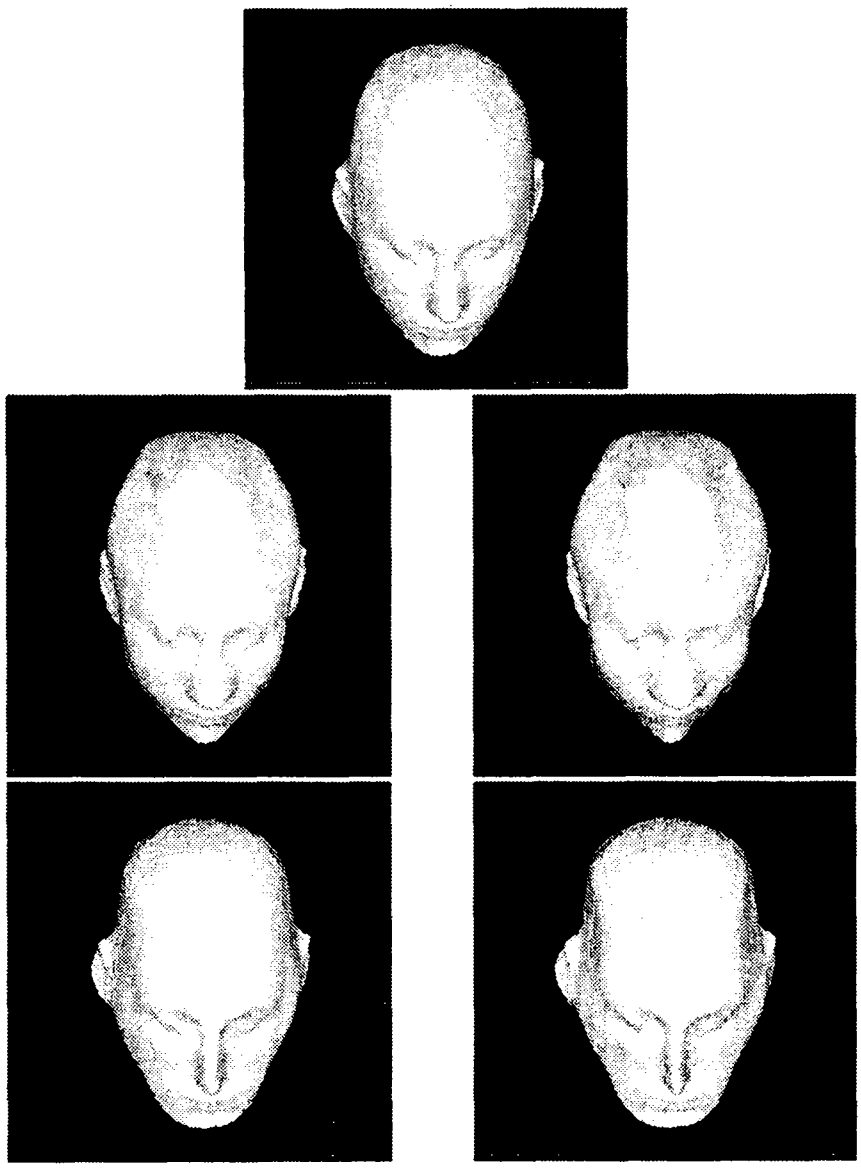

Figure 8: Animating the human head (top, front view) by adding an x-directional mode of sine amplitude

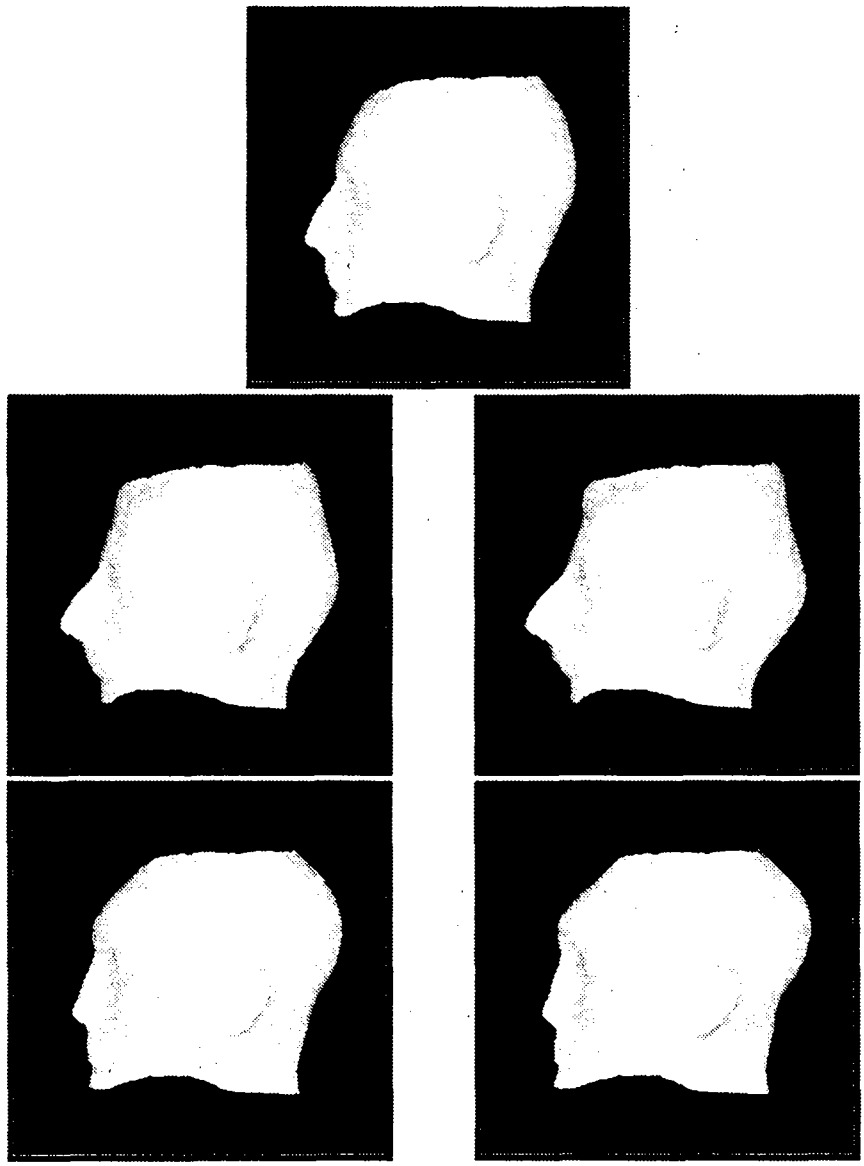

Figure 9: Animating the human head (top, side view) by adding an y-directional mode of sine amplitude

12 Conclusion

We have presented modal dynamics from a new point of view : *the analytic expression of eigenmodes*. Borrowing the solid state physics formulation, we have seen that the harmonic approximation is a sound framework for deriving the equations of motion of our elastically-deformable model.

Then we have developed the analytic expressions of the vibration modes in $2D$ and $3D$, allowing *real time* computations, and we have shown the relationship between modal analysis, Fourier analysis, and wave propagation.

In motion analysis, we have shown the power of modal approximation for a compact description, smoothing and animation of a complex deformation. In computer graphics, modes can be used in the same way, and a real human head (originally magnetic resonance data) is animated.

Acknowledgements

I wish to thank Nicholas Ayache for helpful discussions on the method's possibilities and applications, Maylise Nastar from CEA Saclay for several discussions on Solid State Physics and for providing several references, and Alexis Gourdon who helped with the initial analytic expression of eigenmodes. Thanks are also due to Siemens France and Sopha Medical France for providing the head and the heart data.

This work was supported in part by a grant from Digital Equipment Corporation.

References

[1] Neil W. Ashcroft and M. David Mermin. *Solid State Physics.* Saunders College Publishing International Edition, 1976.

[2] Klaus-Jurgen Bathe. *Finite Element Procedures in Engineering Analysis.* Prentice-Hall, 1982.

[3] Charles Kittel. *Introduction to Solid State Physics.* John Wiley and Sons, 1976. Fifth Edition.

[4] A.A. Maradudin, E.W. Montroll, G.H. Weiss, and I.P. Ipatova. *Theory of Lattice Dynamics in the Harmonic Approximation.* Academic Press, 1971. Second Edition.

[5] Chahab Nastar and Nicholas Ayache. Fast segmentation, tracking, and analysis of deformable objects. Technical Report 1783, INRIA, October 1992.

[6] Chahab Nastar and Nicholas Ayache. Fast segmentation, tracking, and analysis of deformable objects. In *Proceedings of the Fourth International Conference on Computer Vision (ICCV '93)*, Berlin, May 1993.

[7] Chahab Nastar and Nicholas Ayache. *A New Physically Based Model for Efficient Tracking and Analysis of Deformations.* Lecture notes in computer science : Geometric Reasoning - from Perception to Action. Springer-Verlag, 1993.

[8] Chahab Nastar and Nicholas Ayache. Non-rigid motion analysis in medical images : a physically based approach. In *Proceedings of the 13th International Conference on Information Processing in Medical Imaging (IPMI '93)*, Tucson, Arizona, June 1993.

[9] G.N Pande, G. Beer, and J.R. Williams. *Numerical Methods in Rock Mechanics*. John Wiley and Sons, 1990.

[10] A. Pentland and Williams J. The perception of non-rigid motion : Inference of material properties and force. In *Proceedings of the International Joint Conference on Artificial Intelligence*, August 1989.

[11] Alex Pentland and Stan Sclaroff. Closed-form solutions for physically based shape modelling and recognition. *IEEE Transactions on Pattern Analysis and Machine Intelligence*, PAMI-13(7):715–729, July 1991.

[12] Stan Sclaroff and Alex Pentland. Generalized implicit functions for computer graphics. *Computer Graphics*, 25(4):247–250, July 1991.

[13] G. L. Scott. The alternative snake - and other animals. In *Proceedings of the Alvey Vision Conference*, pages 341 – 347, 1987. Cambridge, England.

[14] Lawrence H. Staib and James S. Duncan. Parametrically deformable contour models. In *Proc. Computer Vision and Pattern Recognition*, pages 98–103, 1989.

[15] Lawrence H. Staib and James S. Duncan. Deformable fourier models for surface finding in 3-D images. In *Proceedings of Visualization in Biomedical Computing*, Chapell Hill,USA, October 1992.

Unité de Recherche INRIA Rocquencourt
Domaine de Voluceau - Rocquencourt - B.P. 105 - 78153 LE CHESNAY Cedex (France)

Unité de Recherche INRIA Lorraine Technopôle de Nancy-Brabois - Campus Scientifique
615, rue du Jardin Botanique - B.P. 101 - 54602 VILLERS LES NANCY Cedex (France)
Unité de Recherche INRIA Rennes IRISA, Campus Universitaire de Beaulieu 35042 RENNES Cedex (France)
Unité de Recherche INRIA Rhône-Alpes 46, avenue Félix Viallet - 38031 GRENOBLE Cedex (France)
Unité de Recherche INRIA Sophia Antipolis 2004, route des Lucioles - B.P. 93 - 06902 SOPHIA ANTIPOLIS Cedex (France)

EDITEUR
INRIA - Domaine de Voluceau - Rocquencourt - B.P. 105 - 78153 LE CHESNAY Cedex (France)

ISSN 0249 - 6399